

UNIVERSAL PHASE DIAGRAM AND SCALING FUNCTIONS OF IMBALANCED FERMI GASES

*B. Frank, J. Lang, W. Zwerger**

*Physik-Department, Technische Universität München
D-85748, Garching, Germany*

Received April 9, 2018

Contribution for the JETP special issue in honor of L. P. Pitaevskii's 85th birthday

DOI: 10.1134/S0044451018110020

We consider Fermi gases near a Feshbach resonance close to the unitary regime, where the scattering length a diverges [1, 2]. Using scaling arguments and a Luttinger–Ward approach, we determine the phase diagram in the presence of a finite imbalance between the two spin components $\sigma = \uparrow, \downarrow$ (for reviews of this subject see [3] or the chapters by Chevy and Salomon or by Recati and Stringari in [4]).

In the low density limit $k_F r_e \rightarrow 0$, the finite range of the interactions becomes irrelevant. The effective Hamiltonian

$$\hat{H} = \int_{\mathbf{x}} \left[\sum_{\sigma} \hat{\psi}_{\sigma}^{\dagger}(\mathbf{x}) \left(-\frac{\hbar^2}{2m} \nabla^2 \right) \hat{\psi}_{\sigma}(\mathbf{x}) + \bar{g}(\Lambda) \hat{\psi}_{\uparrow}^{\dagger}(\mathbf{x}) \hat{\psi}_{\downarrow}^{\dagger}(\mathbf{x}) \hat{\psi}_{\downarrow}(\mathbf{x}) \hat{\psi}_{\uparrow}(\mathbf{x}) \right] \quad (1)$$

thus involves a delta function interaction $V(\mathbf{x}) \rightarrow \bar{g}(\Lambda) \delta(\mathbf{x})$ between Fermions of opposite spin. For finite values \bar{g} , the associated scattering amplitude vanishes. Thus $\bar{g}(\Lambda)$ must be adjusted properly to give rise to a non-vanishing physical coupling constant $g = 4\pi\hbar^2 a/m$. This leads to

$$\frac{1}{\bar{g}} = \frac{1}{g} - \int_{q < \Lambda} \frac{1}{2\varepsilon_q}. \quad (2)$$

Here, $\varepsilon_q = \hbar^2 q^2 / 2m$ is the energy of a free particle and the divergent integral is regularized by a cutoff $\Lambda \simeq \pi/\bar{a}$ inversely proportional to the mean scattering length \bar{a} , which determines the effective range of open channel dominated Feshbach resonances.

The ground state of attractive, two-component Fermi gases in the low density limit turns out to be fundamentally different, depending on whether the associated scattering length a is positive or negative. For $a > 0$, the existence of a two-body bound state with energy $\varepsilon_b = \hbar^2/ma^2$ implies that a finite density of Fermions appears — as a dilute gas of dimers — already for a negative (Fermion) chemical potential $\mu > -\varepsilon_b/2$. Since the effective interaction between two dimers is repulsive with scattering length $a_{dd} = 0.6a$ [5], one obtains a stable, dilute BEC. According to the Gross–Pitaevskii equation, its density vanishes linearly as $\mu + \varepsilon_b/2 \rightarrow 0^+$. For negative values of a , there is no bound state. A finite density of Fermions thus only appears for $\mu > 0$, with $n(\mu, T = 0) \sim \mu^{3/2}$ to leading order. Due to the attractive interaction, there is a pairing instability and the ground state is again a superfluid. In the low density regime $\mu \ll \hbar^2/ma^2$, which implies $k_F|a| \ll 1$, the superfluid is of the BCS-type. The situation is fundamentally different if the scattering length is infinite. There, lowering the density or chemical potential from a finite value towards zero, one never reaches a dilute gas of either Bosons or Fermions. Instead, the problem remains a strong coupling one for arbitrary small values of the density. As discussed first by Nikolić and Sachdev [6], the unitary Fermi gas at zero density realizes a novel quantum multicritical point with associated universal scaling functions.

A convenient representation for the scaling functions associated with the unstable fixed point at $\mu = 1/a = h = 0$ is obtained within a grand canonical description, where both the total particle number $\hat{N} = \hat{N}_{\uparrow} + \hat{N}_{\downarrow}$ and the “polarization” $\hat{S} = \hat{N}_{\uparrow} - \hat{N}_{\downarrow}$ are controlled by their conjugate thermodynamic variables μ and h . The associated partition function

* E-mail: zwerger@ph.tum.de

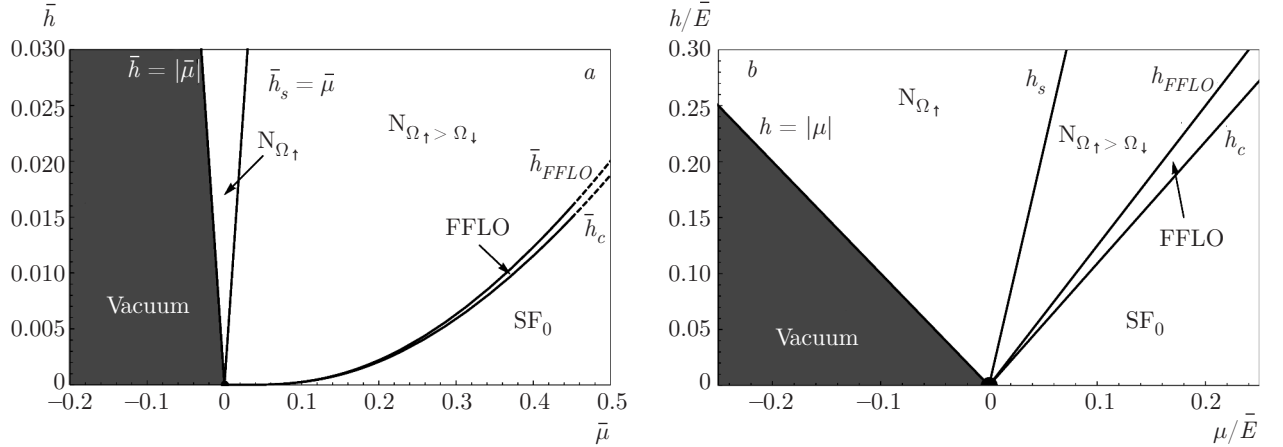


Fig. 1. Panel *a*): Universal phase diagram for negative values of $1/a$ with the finite density phases: fully polarized gas $N_{\Omega_{\uparrow}}$, normal fluid with finite spin population of the minority atoms $N_{\Omega_{\uparrow} > \Omega_{\downarrow}}$, and the superfluid FFLO and balanced BCS phase, the latter denoted as SF_0 . The dashed lines indicate the crossover of the critical fields towards the strong coupling regime. Panel *b*): Unitary limit of the universal phase diagram, where all phase boundaries extend linearly from the quantum multicritical point.

Note that the slopes of h_c and h_{FFLO} represent the Luttinger–Ward results

$$\begin{aligned} Z_V(\beta, \mu, h, 1/a) &= \text{Tr} \exp \left\{ -\beta \left(\hat{H} - \mu \hat{N} - h \hat{S} \right) \right\} = \\ &= \exp(V\beta p) \quad (3) \end{aligned}$$

determines the pressure p , from which the total density $n = n_{\uparrow} + n_{\downarrow}$ and the spin density $s = n_{\uparrow} - n_{\downarrow}$ follow by differentiation $n = \partial p / \partial \mu$ and $s = \partial p / \partial h$. Its dependence on the three relevant scaling variables μ , h , and $1/a$ can be expressed in terms of a universal function $f_p(x, y, z)$. A convenient definition is obtained by factorizing out the pressure $p^{(0)}(T, \mu)$ of a balanced two-component, non-interacting Fermi gas in the form

$$p(T, \mu, h, 1/a) = p^{(0)}(T, \mu) f_p \left(\beta \mu, \beta h, \frac{\lambda_T}{a} \right), \quad (4)$$

where $\lambda_T = \hbar \sqrt{2\pi/mT}$ is the thermal wavelength (we use units for the temperature where $k_B = 1$). For the special case of a balanced, unitary gas, the function $f_p(\beta\mu, 0, 0)$ has been determined experimentally from an integration of the directly measured density $n(\beta, \mu)$ in the relevant range between the non-degenerate limit at $\beta\mu \simeq -1.6$ down to [7] and also below the superfluid transition at $(\beta\mu)_c \simeq 2.5$ [8]. Its extension to finite values of h will be calculated below, using the Luttinger–Ward formalism in the normal fluid regime.

At zero temperature, the scaling function depends on two variables only, which is reduced further to the single variable h/μ right at unitarity. For finite values of the scattering length, both positive or negative, a convenient choice for the two scaling variables are the dimensionless chemical potential $\bar{\mu} = \mu/(\varepsilon_b/2)$ and the

dimensionless Zeeman field $\bar{h} = h/(\varepsilon_b/2)$. Factorizing out $p^{(0)}(0, \mu) \sim \mu(2m\mu)^{3/2}/h^3$, the scaling functions at zero temperature may then be defined by

$$\frac{p(\mu, h, 1/a)}{p^{(0)}(0, \mu)} = f_{\pm}(\bar{\mu}, \bar{h}) \rightarrow f(h/\mu) \text{ at } 1/a = 0, \quad (5)$$

where the subscript \pm differentiates between positive or negative values of $1/a$. In particular, the value $f(0) = \xi_s^{-3/2} \simeq 4.44$ of the scaling function, which characterizes the ground state of the balanced Fermi gas at unitarity, is fixed by the Bertsch parameter $\xi_s \simeq 0.37$.

The universal phase diagrams at zero temperature and finite values of the field h are shown in Fig. 1, both for the unitary gas and the one with a negative scattering length. For the unitary gas, the vacuum state at $\mu < 0$ evolves into a fully polarized Fermi gas at $h = |\mu|$. The same state can also be reached for $\mu > 0$, provided $h > h_s$ is larger than a “saturation field” h_s beyond which the Fermi gas is fully polarized. As realized by Chevy [9], this field is determined by calculating the addition energy of a single down spin added to a Fermi sea of up spins. A precise solution of the associated Fermi polaron problem shows that the ratio $\eta = \mu_{\downarrow}/\mu_{\uparrow} = -0.615$ of the chemical potentials has a universal value at unitarity [10]. Due to

$$\eta = \frac{\mu_{\downarrow}}{\mu_{\uparrow}} = \frac{1 - h/\mu}{1 + h/\mu} \leq 1 \quad (6)$$

this ratio fixes the corresponding saturation field $(h/\mu)_s = (1 - \eta_s)/(1 + \eta_s) = 4.19$. Starting from

small values of the field h , the gapped superfluid at $h = 0$ acquires a finite polarization $s \neq 0$ beyond a Clogston–Chandrasekhar (CC) field h_c [11, 12]. From our Luttinger–Ward calculation below, this field is at $(h/\mu)_c = 1.09 \pm 0.05$. Regarding the nature of the ground state in the regime $h_c < h < h_s$, the simplest assumption is that it is a normal Fermi liquid with two Fermi surfaces. Their volumes $\Omega_{\uparrow,\downarrow}$ in momentum space are connected with the finite polarization $s \neq 0$ by the exact relation

$$s = \frac{\Omega_\uparrow - \Omega_\downarrow}{(2\pi)^3} \quad (7)$$

derived, for homogeneous phases, by Sachdev and Yang [13]. Our results below indicate, however, that an intermediate inhomogeneous superfluid with FFLO-order appears beyond the CC-limit since the vertex associated with s-wave pairing diverges at a finite rather than at zero center of mass momentum Q at the lowest accessible temperatures in the regime immediately above h_c . From our numerical results below we estimate a critical value $(h/\mu)_{FFLO} = 1.28 \pm 0.15$. The ground state beyond h_{FFLO} , which again has two Fermi surfaces, is likely to be unstable to p-wave pairing around the majority Fermi surface as discussed by Kagan and Chubukov for imbalanced Fermi gases with repulsive interactions in the regime $k_F a \ll 1$ [14], see also [15]. For the following discussion, we will neglect this and assume it is a Fermi liquid state, as indicated experimentally [16]. The resulting phase diagram is shown in Fig. 1b. Apart from the vacuum transition line $h = |\mu|$, it features three straight lines which, as a consequence of scale invariance, are perfectly linear up to the cutoff energy $\bar{E} \simeq \hbar^2/mr_e^2$. Their slopes are universal numbers, which are just the values of h/μ where the scaling function $f(h/\mu)$ defined in (5) exhibits singularities. In particular, at the first order CC-transition, $f(h/\mu)$ has a discontinuity in slope from zero below $(h/\mu)_c$ to a positive value above.

The h versus μ phase diagram at negative values of the scattering length is determined by the fact that the limit $\mu \ll \hbar^2/ma^2$ corresponds to a Fermi superfluid of the BCS-type, with a crossover to the strong coupling fixed point for $\bar{\mu} = \mu/(\varepsilon_b/2) = \mathcal{O}(1)$. Indeed, the line $\mu = 0$ at finite negative values of $1/a$ is a line of quantum critical points which all share the same fixed point, namely a weak coupling BCS superfluid.

In the limit $\bar{\mu} \ll 1$, the boundary of the balanced superfluid phase is thus given by the standard result $h_c = \Delta/\sqrt{2}$ [17, 18], which yields

$$\bar{h}_c(\bar{\mu} \ll 1) = \bar{\mu} \frac{(2/e)^{7/3}}{\sqrt{2}} \exp(-\pi/2\sqrt{\bar{\mu}}), \quad (8)$$

where we have used the exact expression for the gap Δ [19]. This line extends in a continuous manner to the strong coupling regime $\bar{\mu} \gg 1$, where $(h/\mu)_c \simeq 1.09$ approaches the strictly linear behavior at the unitary fixed point. The fact that the CC-line extends in a continuous manner up to unitarity and even beyond to positive scattering lengths is connected with the fact that the so called splitting point S , below which the transition from a balanced to a polarized superfluid with a finite Fermi surface of majority atoms is no longer continuous [20], is on the BEC side at $1/a > 0$. Beyond the CC-transition, a weak coupling Fermi gas turns into an inhomogeneous superfluid with an order parameter which varies periodically like $\cos(\mathbf{Q} \cdot \mathbf{x})$. This phase, which is denoted generically by FFLO in the following, is the ground state in a small window $1/\sqrt{2} < h/\Delta < 0.754$ [21, 22]. It defines an FFLO-line $h_{FFLO}(\bar{\mu} \ll 1) = 0.754\Delta$ just above the CC-line (8) with the same dependence on $\bar{\mu}$. For $\bar{\mu} \gg 1$, this line again acquires the linear dependence $(h/\mu)_{FFLO} \simeq 1.28$ characteristic for the behavior at unitarity. Similarly, the saturation field h_s beyond which only a single Fermi surface remains, has a simple form $h_s(\bar{\mu} \ll 1) = \mu$ in the weak coupling limit, because pairing is suppressed exponentially. Thus, to leading order, the saturation field is given by its value in a non-interacting Fermi gas. For $\bar{\mu} \gg 1$, in turn, the dependence is again linear, but the slope is now given by the universal number 4.19 which characterizes the strong coupling fixed point discussed above. The complete phase diagram is shown in Fig. 1a, restricted to the regime $\bar{\mu} \ll 1$. The smooth crossover between the weak and strong coupling fixed points discussed above shows that, using the proper dimensionless units $\bar{\mu}$ and \bar{h} , this diagram is the universal phase diagram for all negative values of the scattering length. Arbitrary values of $1/a < 0$ can thus be collapsed into a single diagram whose behavior is known quantitatively in both the weak and strong coupling limit $\bar{\mu} \ll 1$ or $\bar{\mu} \gg 1$. An equivalent result also holds for positive scattering lengths. The associated universal phase diagram is, however, more complicated, as discussed qualitatively by Son and Stephanov [20].

Luttinger–Ward theory. For a quantitative study of the thermodynamics at finite temperature, we use a diagrammatic approach in which the grand potential $\Omega(T, \mu, h, 1/a, V) = -pV$ which directly determines the pressure p , is represented in terms of the formally exact Luttinger–Ward functional [23]

$$\Omega[G] = \beta^{-1} (\text{Tr}\{\ln[G] + [1 - G_0^{-1}G]\} + \Phi[G]). \quad (9)$$

Here, $G = \{\mathcal{G}_\uparrow, \mathcal{G}_\downarrow\}$ denotes the two independent components of the interacting Green function and $G_0 = \{\mathcal{G}_{\uparrow,0}, \mathcal{G}_{\downarrow,0}\}$ contains the bare Green functions

$$\mathcal{G}_{\sigma,0}(\mathbf{k}, \omega_n) = \frac{1}{i\hbar\omega_n - (\varepsilon_k - \mu_\sigma)}, \quad (10)$$

which involve fermionic Matsubara frequencies $\hbar\omega_n = 2\pi(n + 1/2)T$. Since we only consider the normal phase, no anomalous expectation values appear. Moreover, we restrict ourselves to s-wave pairing in a relative singlet configuration. The vertex function Γ thus only depends on a single momentum and frequency. In the zero range limit, Γ is a scalar in spin space, which contains only the center of mass dynamics of the pairs

$$\begin{aligned} \Gamma(\mathbf{x}, \tau) &= \bar{g}(\Lambda) \delta(\tau) \delta(\mathbf{x}) - \\ &- \bar{g}^2(\Lambda) \langle \mathcal{T} \left(\hat{\psi}_\downarrow \hat{\psi}_\uparrow \right) (\mathbf{x}, \tau) \times \\ &\times \left(\hat{\psi}_\uparrow^\dagger \hat{\psi}_\downarrow^\dagger \right) (\mathbf{0}, 0) \rangle. \end{aligned} \quad (11)$$

Its short distance and short time limit determines the Tan contact density

$$\begin{aligned} \frac{\hbar^4}{m^2} \mathcal{C} &= -\Gamma(\mathbf{x} = \mathbf{0}, \tau = 0^-) = \\ &= -\lim_{\Lambda \rightarrow \infty} \bar{g}^2(\Lambda) \langle \hat{\psi}_\uparrow^\dagger(\mathbf{x}) \hat{\psi}_\downarrow^\dagger(\mathbf{x}) \hat{\psi}_\downarrow(\mathbf{x}) \hat{\psi}_\uparrow(\mathbf{x}) \rangle, \end{aligned} \quad (12)$$

which also appears in the Tan pressure relation [24]

$$p = \frac{2}{3} \varepsilon + \frac{\hbar^2}{12\pi ma} \mathcal{C} \quad (13)$$

connecting pressure p and energy density ε . The non-trivial part Φ of the Luttinger–Ward functional determines the spin-dependent self-energy

$$\Sigma_\sigma[G] = \frac{\delta\Phi[G]}{\delta\mathcal{G}_\sigma}. \quad (14)$$

The full Green function then follows by solving the self-consistent Dyson equation

$$\mathcal{G}_\sigma^{-1} = \mathcal{G}_{\sigma,0}^{-1} - \Sigma_\sigma[G]. \quad (15)$$

Specifically, we constrain Φ to the particle–particle ladder. For a balanced Fermi gas at $h = 0$, both the critical temperature $T_c/T_F \simeq 0.16$ and the Bertsch parameter $\xi_s = 0.36$ at $T = 0$, obtained in this manner [25], agree very well with the corresponding experimental values [8]. Within this approximation, the vertex function can be written in the form

$$\Gamma(\mathbf{Q}, \Omega_n) = \frac{1}{1/g + M(\mathbf{Q}, \Omega_n)}, \quad (16)$$

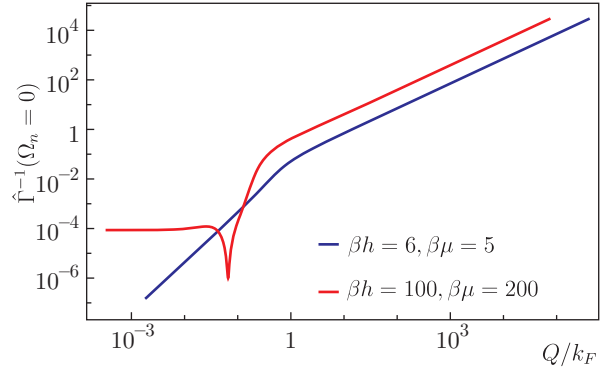


Fig. 2. (Color online) Double logarithmic plot of two typical critical inverse vertices. Blue line: Phase transition to a homogeneous superfluid. Red line: Phase transition to an FFLO state with finite \mathbf{Q}

where

$$\begin{aligned} M(\mathbf{Q}, \Omega_n) &= \int \frac{d^3 k}{(2\pi)^3} \times \\ &\times \left[\frac{1}{\beta} \sum_m \mathcal{G}_\uparrow(\mathbf{k}, \omega_m) \mathcal{G}_\downarrow(\mathbf{Q} - \mathbf{k}, \Omega_n - \omega_m) - \frac{1}{2\varepsilon_k} \right]. \end{aligned} \quad (17)$$

The self-energy is connected with the vertex and the exact Green function via

$$\begin{aligned} \Sigma_\sigma(\mathbf{k}, \omega_n) &= \int \frac{d^3 Q}{(2\pi)^3} \frac{1}{\beta} \times \\ &\times \sum_m \Gamma(\mathbf{Q}, \Omega_m) \mathcal{G}_{\bar{\sigma}}(\mathbf{Q} - \mathbf{k}, \Omega_m - \omega_n), \end{aligned} \quad (18)$$

where $\bar{\sigma}$ is the spin orientation complementary to σ . Together with (15) and (16), this gives a closed set of equations for the Green functions $\mathcal{G}_\sigma(\mathbf{k}, \omega_n)$.

The equations (16)–(18) together with the Dyson equation (15) are solved numerically in an iterative manner, until convergence for each set of initial, dimensionless parameters $\beta\mu, \beta h$ and λ_T/a has been reached. The instability to the formation of a superfluid is signaled by a zero of the inverse vertex. In the standard case of pairing with vanishing center of mass momentum, we locate the transition point in parameter space by the criterion that $\Gamma^{-1}(\mathbf{Q} \rightarrow \mathbf{0}, \Omega_n = 0) \sim \mathbf{Q}^2$ approaches zero like the square of the center of mass momentum [26]. The quadratic behavior in \mathbf{Q} is well resolved in our numerical data, as shown in Fig. 2. For large momenta, we obtain a linear behavior $\Gamma^{-1}(\mathbf{Q}, \Omega_n = 0) \sim |\mathbf{Q}|$ which is characteristic for a zero range interaction with a finite value of the contact density \mathcal{C} defined in (12). In the regime where an

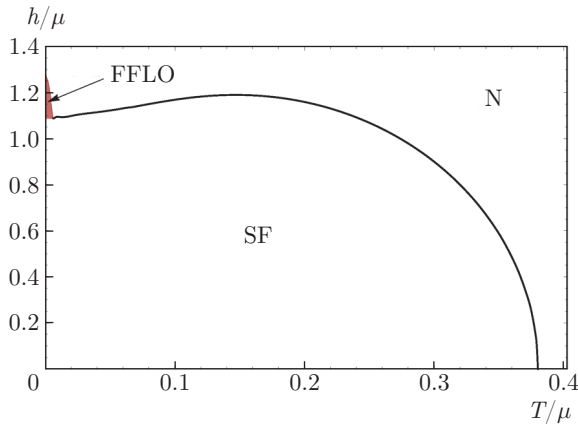


Fig. 3. (Color online) Phase diagram at unitarity. The extrapolation to $T = 0$ yields $(h/\mu)_c = 1.09 \pm 0.05$. At very small T and $h > h_c$ FFLO order (red shaded) emerges

instability of the FFLO-type dominates, we accept a threshold of $|\hat{\Gamma}^{-1}(\mathbf{Q}, \Omega_n = 0)| \leq 10^{-6}$, for the dimensionless inverse vertex $\hat{\Gamma}^{-1} \equiv -(2\pi)^{3/2} \lambda_T^3 \Gamma^{-1}/\beta$ at a finite value of \mathbf{Q} as zero. To check the precision of our numerical results, we compute the pressure from the grand potential in equation (9) and compare it to the Tan pressure relation (13). The resulting relative deviations are typically around 10^{-4} .

The phase diagram of the unitary gas at finite temperature is shown in Fig. 3. The critical temperature at vanishing field $h = 0$ is $(T/\mu)_c \simeq 0.38$, which corresponds to $T_c/T_F \simeq 0.15$. Apparently, at temperatures below $T/\mu \simeq 0.15$ the critical field $(h/\mu)_c$ starts to decrease slightly. This unexpected behavior is due to the presence of a tricritical point, below which the normal to superfluid transition is of first order. The present approach, which is restricted to the normal fluid, can only determine the lower critical field, at which the normal state ceases to be at least metastable. To faithfully determine the position of this tricritical point, and the critical field below it, requires a calculation which includes the symmetry broken phase. This will be presented in future work. At very low temperatures, we find a regime where the instability occurs at a finite wave vector. An extrapolation to the lowest available temperatures shows that $(h/\mu)_{FFLO} = 1.28 \pm 0.15$. Our extrapolated value $(h/\mu)_c = 1.09 \pm 0.05$ for the CC-transition of the unitary gas is considerably larger than the one obtained by Lobo et al. [27], where $(h/\mu)_c = 0.96$, and also in the more recent work by Boettcher et al. [28], who obtain $(h/\mu)_c = 0.83$. Experimentally, the ratio has been inferred from in situ imaging of the density profiles in a trapped imbalanced gas by Shin et al. [29]. In par-

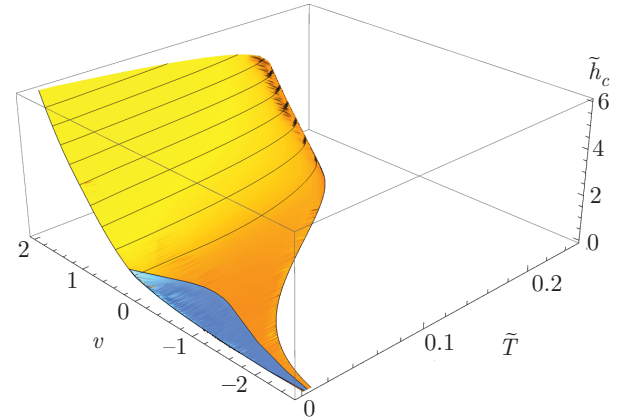


Fig. 4. (Color online) Critical field $(h/\varepsilon_F)_c$ as a function of T/T_F and inverse scattering length v . Yellow: Transition to homogeneous superfluid, Blue: FFLO state with largest $T_c/T_F \simeq 0.03$ near $v \simeq -0.75$

ticular, it has been shown there that the parameter η_c in $(h/\mu)_c = (1 - \eta_c)/(1 + \eta_c)$ can be connected to the measured ratio R_c/R_\uparrow of the radius R_c of the balanced superfluid in the center of the trap and the outer radius R_\uparrow of the fully polarized gas at the edge by the relation

$$\eta_c = \frac{2 \left[\xi_s (n_s(0)/n_0)^{2/3} - 1 \right]}{1 - (R_c/R_\uparrow)^2} + 1. \quad (19)$$

Apart from the universal Bertsch parameter ξ_s , it only contains the ratio between the central density $n_s(0)$ of the balanced superfluid and the density n_0 of a fully polarized Fermi gas with chemical potential $\mu_\uparrow(0)$. The measured values $R_c/R_\uparrow = 0.43$ and $n_s(0)/n_0 = 1.72$ for the coldest sample then give $\eta_c = 0.03$ or $(h/\mu)_c = 0.95$ with a Bertsch parameter $\xi_s = 0.42$. Using the precise result $\xi_s = 0.37$, however, leads to the much larger $(h/\mu)_c = 1.35$. A possible explanation for the discrepancy with the result $(h/\mu)_c = 1.09$ found here is that the effective Bertsch parameter at the finite temperature of the experiment is higher than the universal value at $T = 0$. A rather small critical field $(h/\mu)_c = 0.88$ has also been inferred in later measurements by Navon et al. [30], but again the value changes substantially if the precise number of the Bertsch parameter is used rather than the assumed value $\xi_s = 0.42$.

Finally, in Fig. 4, we show the critical field strength $\tilde{h}_c = (h/\varepsilon_F)_c$ as a function of the reduced temperature $\tilde{T} = T/T_F$ and the dimensionless interaction strength $v = 1/(k_F a)$ in the crossover regime $|v| < 2$. While the line of critical temperatures for the balanced gas $T_c(\tilde{h} = 0)/T_F$ coincides with previous results, we generally observe decreasing values of the critical temperatures with growing Zeeman field. The FFLO-wedge

extends from the BCS limit to the unitary regime with a maximum in the transition temperature on the order of $0.03 T_F$ for interaction strengths $v \simeq -0.75$ slightly on the BCS side of the unitary limit.

To conclude, we have reanalyzed the basic problem of Fermi gases with a finite Zeeman field. In the context of ultracold atoms, where the relevant range is the one near infinite scattering length, quantitatively reliable results for the thermodynamic functions at finite temperature for this problem are still rare. Based on an extension of an earlier Luttinger–Ward approach to finite imbalance, our results provide strong evidence for the presence of an FFLO phase for Fermi gases near unitarity, consistent with the rather general, non-perturbative argument given by Son and Stephanov [20]. The associated critical temperatures are unfortunately rather small, with a maximum of order $\simeq 0.03 T_F$ slightly on the BCS side of the unitary gas. Of course, a detailed analysis of the various symmetry broken phases is still open. In particular, it seems important to study both the precise position and the thermodynamic phases near the splitting point, where the quasiparticle dispersion of the balanced superfluid changes its nature.

This paper is dedicated to Lev Pitaevskii, to whom W. Z. is grateful for discussions and insightful remarks on the physics of ultracold atoms and beyond during many years. We also acknowledge financial support of this work by the Nano-Initiative Munich (NIM).

The full text of this paper is published in the English version of JETP.

REFERENCES

1. M. W. Zwierlein, in *Novel Superfluids*, ed. by K. H. Bennemann and J. B. Ketterson, Vol. 2, Oxford Sci. Publ., Oxford (2014), pp. 269–422.
2. W. Zwerger, in *Quantum Matter at Ultralow Temperatures, Proc. Int. School of Physics “Enrico Fermi”*, ed. by M. Inguscio, W. Ketterle, S. Stringari, and G. Roati, Course 191, Varenna, July 2014, IOS Press, Amsterdam (2016), pp. 63–141.
3. F. Chevy and C. Mora, Rep. Progr. Phys. **73**, 112401 (2010).
4. *The BCS-BEC Crossover and the Unitary Fermi Gas*, ed. by W. Zwerger, Lecture Notes in Physics, Vol. 836, Springer, Berlin, Heidelberg (2012).
5. D. S. Petrov, C. Salomon, and G. V. Shlyapnikov, Phys. Rev. Lett. **93**, 090404 (2004).
6. P. Nikolić and S. Sachdev, Phys. Rev. A **75**, 033608 (2007).
7. K. Van Houcke, F. Werner, E. Kozik et al., Nature Phys. **8**, 366 (2012).
8. M. J. H. Ku, A. T. Sommer, L. W. Cheuk, and M. W. Zwierlein, Science **335**, 563 (2012).
9. F. Chevy, Phys. Rev. A **74**, 063628 (2006).
10. N. Prokof’ev and B. Svistunov, Phys. Rev. B **77**, 020408 (2008).
11. M. W. Zwierlein, A. Schirotzek, C. H. Schunck, and W. Ketterle, Science **311**, 492 (2006).
12. G. B. Partridge, W. Li, R. I. Kamar et al., Science **311**, 503 (2006).
13. S. Sachdev and K. Yang, Phys. Rev. B **73**, 174504 (2006).
14. M. Y. Kagan and A. V. Chubukov, JETP Lett. **50**, 483 (1989).
15. M. A. Baranov, Y. Kagan, and M. Y. Kagan, JETP Lett. **64**, 273 (1996).
16. S. Nascimbène, N. Navon, S. Pilati et al., Phys. Rev. Lett. **106**, 215303 (2011).
17. B. S. Chandrasekhar, Appl. Phys. Lett. **1**, 7 (1962).
18. A. M. Clogston, Phys. Rev. Lett. **9**(6), 266 (1962).
19. L. P. Gor’kov and T. K. Melik-Barkhudarov, Zh. Eksp. Teor. Fiz. **40**, 1452 (1961).
20. D. T. Son and M. A. Stephanov, Phys. Rev. A **74**, 013614 (2006).
21. P. Fulde and R. A. Ferrell, Phys. Rev. A **135**, 550 (1964).
22. A. I. Larkin and Y. N. Ovchinnikov, Zh. Eksp. Teor. Fiz. **47**, 1136 (1964).
23. J. M. Luttinger and J. C. Ward, Phys. Rev. **118**, 1417 (1960).
24. S. Tan, Ann. Phys. **12**, 2987 (2008).
25. R. Haussmann, W. Rantner, S. Cerrito, and W. Zwerger, Phys. Rev. A **75**, 023610 (2007).
26. A. A. Abrikosov, L. P. Gor’kov, and I. E. Dzyaloshinskii, *Methods of Quantum Field Theory in Statistical Physics*, Dover Publ., New York (1975).

27. C. Lobo, A. Recati, S. Giorgini, and S. Stringari, Phys. Rev. Lett. **97**, 200403 (2006).
28. I. Boettcher, J. Braun, T. K. Herbst et al., Phys. Rev. A **91**, 013610 (2015).
29. Y. Shin, C. H. Schunck, A. Schirotzek, and W. Ketterle, Nature, **451** (7284), 689 (2008).
30. N. Navon, S. Nascimbène, F. Chevy, and C. Salomon, Science **328**, 729 (2010).